A Novel Nonobese Diabetic/Severe Combined Immunodeficient Xenograft Model for Chronic Lymphocytic Leukemia Reflects Important Clinical Characteristics of the Disease

Jan Dürig,[1] Peter Ebeling,[2] Florian Grabellus,[3] Ursula R. Sorg,[2] Michael Möllmann,[2] Philipp Schütt,[2] Joachim Göthert,[1] Ludger Sellmann,[1,4] Siegfried Seeber,[2] Michael Flasshove,[2] Ulrich Dührsen,[1] and Thomas Moritz[2,5]

Departments of [1]Hematology, [2]Internal Medicine (Cancer Research), and [3]Pathology and Neuropathology, and [4]Institute of Cell Biology, University of Duisburg-Essen Medical School, Essen, Germany and [5]Division of Experimental Hematology, Cincinnati Children's Hospital Medical Center, Cincinnati, Ohio

Abstract

We here describe a novel xenograft model of chronic lymphocytic leukemia (CLL) generated by infusion of human primary CLL cells into immunodeficient nonobese/severe combined immunodeficient (NOD/SCID) mice. Combined i.v. and i.p. injection of peripheral blood mononuclear cells (PBMC) from 39 patients with CLL resulted in highly reproducible splenic (37 of 39) and peritoneal (35 of 39) engraftment, which remained stable over a time span of 4 to 8 weeks. By comparison, recovery of leukemic cells from bone marrow (21 of 39) or peripheral blood (8 of 22) was substantially lower. The engraftment pattern of CLL PBMC 4 weeks posttransplant was correlated with clinical disease activity: infusion of PBMC from donors with Binet stage A, lymphocyte doubling time of >12 months, and normal lactate dehydrogenase (LDH) serum levels led to marked engraftment of T cells whereas comparably few tumor cells could be detected. In contrast, NOD/SCID mice receiving PBMC from donors with advanced stage Binet C, lymphocyte doubling time of <12 months, and elevated LDH serum levels exhibited predominant engraftment of tumor cells and comparably low numbers of T cells. These results suggest that this model reflects the heterogeneity and important clinical characteristics of the disease, and thus may serve as a tool for preclinical drug testing and investigation of the pathophysiology of CLL. [Cancer Res 2007;67(18):8653–61]

Introduction

In the past 10 years, several xenograft models of human chronic lymphocytic leukemia (CLL) using immunocompromised severe combined immunodeficient (SCID) mice have been reported (1–4). Work in this field has generally been hampered by inefficient engraftment (1) and EBV transformation of human cells (2). Recently, some of these pitfalls were successfully addressed by Shimoni et al. (3), who transplanted CLL peripheral blood mononuclear cells (PBMC) into the peritoneal cavity of lethally irradiated mice radioprotected with bone marrow from SCID mice. Importantly, in their initial description of this model, the authors found that PBMC from donors with Rai stage 0 disease led to marked engraftment of human T cells but comparably few leukemic B cells. In contrast, chimeric mice receiving PBMC from patients with advanced CLL (Rai stage III and IV) exhibited a reverse engraftment pattern with a predominance of tumor cells over accessory T cells (3). In a follow-up study, the same authors elegantly showed that autologous T cells can control CLL cell engraftment and suggested that their model could provide a useful tool for the investigation of the pathogenesis and disease progression in CLL (4). However, limitations of this approach have also been noted in that engraftment of CLL cells was followed only over a comparably short period of 2 weeks and the site of engraftment was restricted to the peritoneal cavity.

Following up on the above described studies, we aimed at developing a novel xenograft model for human CLL by transplanting primary CLL PBMC into nonobese diabetic (NOD)/SCID mice and analyzing the engraftment potential of these cells in various murine tissues over a time period of up to 12 weeks. Furthermore, the engraftment capacity of CLL cells was correlated with the disease stage and the molecular risk factor profile of the individual donors.

Materials and Methods

Patients and isolation of CLL cells. For establishment and evaluation of the model, peripheral blood samples from 39 CLL patients treated at the University Hospital Essen between December 2004 and December 2006 were used (for details, see Table 1). In all patients, the morphologic diagnosis of CLL was confirmed by flow cytometry revealing a typical $CD19^+CD5^+CD23^+$ immunoglobulin light chain (κ or λ light chain)–restricted immunophenotype. Expression of ZAP-70 and CD38 was determined by flow cytometry as recently described (5). Patient selection was based on a WBC count exceeding 20/nL and a treatment-free interval of ≥6 months before sample acquisition. Heparanized whole-blood cell samples (peripheral blood, 20–50 mL) were obtained during routine follow-up visits to our institutions. Informed consent was obtained according to institutional guidelines. Peripheral blood mononuclear cells (PBMC) were isolated within 3 h of venipuncture by Ficoll-Hypaque (Pharmacia) density centrifugation. The interlayer was collected, washed twice, counted on a hemocytometer, and resuspended in Iscove's modified Dulbecco's medium (IMDM; Life Technologies, Inc.) at the desired cell concentration and transplanted within 2 h. In five experiments, PBMC before transplantation were depleted of $CD3^+$ human T cells using the MidiMACS isolation system (Miltenyi Biotech). Purity of $CD19^+$ cells after T-cell depletion was >99.5% as analyzed by flow cytometry. T cell–depleted grafts were compared with T cell–enriched grafts, in which 0.5×10^7 to 1.9×10^7 T cells (equivalent to 5–18% of total cells and double the amount of T cells present in the original PBMC sample) were added to the grafts before transplantation.

Note: Supplementary data for this article are available at Cancer Research Online (http://cancerres.aacrjournals.org/).

J. Dürig and P. Ebeling contributed equally to this work.

Requests for reprints: Peter Ebeling, Department of Internal Medicine (Cancer Research), University of Duisburg-Essen Medical School, Hufelandstraße 55, 45122 Essen, Germany. Phone: 49-201-723-3120; Fax: 49-201-723-2735; E-mail: peter.ebeling@uni-due.de.

doi:10.1158/0008-5472.CAN-07-1198

Transplantation of NOD/SCID mice. NOD/SCID mice of both genders were bred and handled under sterile condition and animals were transplanted at ages 8 to 15 weeks. PBMC were transplanted into NOD/SCID mice at 30 to 60 min after sublethal irradiation (3.0–3.25 Gy) of the animals using i.v. and/or i.p. application. A total of 1.0×10^8 PBMC suspended in 0.2 mL of IMDM were injected per chosen route.

Collection of cells from NOD/SCID mice. Peripheral blood was obtained every 2 weeks from the tail veins of transplanted animals. For harvest of cells from the peritoneal cavity, bone marrow, and spleen, mice were sacrificed by cervical dislocation 4, 8, or 12 weeks after transplantation or earlier when they became listless or unwell. Peritoneal cells were obtained by peritoneal lavage with 5 mL of 0.9% NaCl whereas bone marrow cells were obtained by flushing the femoral, tibial, and hip bones with IMDM and afterward filtering cells through 70-μm nylon sieves (Becton Dickinson). For analysis of engraftment within the murine spleen, one half of the organ was fixed immediately in buffered 3.7% formalin and afterward embedded in paraffin for further histologic and immunohistochemical analyses. The other half was mechanically homogenized, pressed through 70-μm nylon sieves (BD Falcon), and suspended in PBS for further analysis by flow cytometry.

Characterization of human cell engraftment in NOD/SCID mice using flow cytometry. For detection of cell-surface antigens, single-cell suspensions obtained from the different organs were incubated for 30 min on ice with a mixture of the indicated appropriate fluorescently labeled

Table 1. Patients characteristics

CLL sample	Age (y)	Sex (gender)	Disease activity			Prognostic parameters				WBC (/nL)	Inoculated cells		Transplanted mice (eng/total)
			Stage (Binet)	LDH (units/L)	LDT (mo)	CD38	ZAP-70	IgVH-MStat	Cytogenetics		$CD19^+/CD5^+$ (%)	$CD3^+$ (%)	
1	54	M	A	224	>12	−	+	UM	Normal	75	89.9	5.0	3/3
2	71	F	A	160	>12	−	−	ND	13q-	45	ND	ND	0/1
3	65	M	C	256	ND	+	−	ND	13q-11q-	264	98.0	2.4	2/2
4	49	M	B	ND	ND	−	+	UM	13q-	159	94.5	3.8	2/4
5	56	F	A	265	<12	−	+	M	+12	320	97.8	2.5	3/3
6	75	F	C	210	>12	−	+	UM	13q-17p-	110	97.1	4.3	3/3
7	49	F	A	182	>12	−	−	ND	Normal	70	95.0	8.2	3/5
8	42	M	B	187	>12	+	+	ND	13q-11q-	135	94.6	2.8	4/4
9	51	M	A	ND	ND	+	+	ND	+12	69	97.0	2.0	3/5
10	78	M	A	186	>12	−	−	M	Normal	104	97.3	1.9	4/6
11	75	M	A	219	ND	−	+	M	17p-	96	93.5	4.1	4/4
12	58	F	A	280	ND	−	+	ND	13q-	73	87.8	6.7	3/5
13	70	M	C	533	<12	+	+	ND	+12	156	96.1	2.4	4/4
14	38	M	A	179	>12	−	−	ND	13q-	61	95.0	3.4	2/2
15	51	M	C	200	<12	+	−	UM	17p-	453	92.6	4.5	2/8
16	70	M	A	277	ND	−	−	ND	13q-	32	92.6	4.5	2/2
17	71	M	A	351	>12	−	−	M	13q-	21	ND	ND	0/1
18	55	M	C	196	<12	+	+	UM	13q-17p-	83	95.4	1.5	8/8
19	75	M	B	128	<12	+	+	UM	13q-	133	94.7	4.1	4/6
20	62	M	C	343	>12	−	+	ND	13q-	216	95.7	5.8	2/5
21	53	F	B	269	>12	−	−	ND	13q-	168	96.7	1.8	1/1
22	53	M	B	194	<12	+	+	UM	+12	59	93.0	3.1	3/3
23	72	M	C	350	<12	+	+	M	13q-	47	94.4	3.9	3/4
24	61	M	A	209	<12	+	−	ND	ND	180	95.7	2.4	4/4
25	50	F	A	225	>12	+	+	UM	13q-	ND	92.7	6.2	4/4
26	52	M	A	164	>12	−	+	UM	ND	42	90.8	4.3	3/4
27	80	F	A	283	>12	−	ND	ND	13q-	81	91.7	4.3	3/3
28	38	F	B	189	<12	+	+	UM	Normal	92	95.5	3.0	1/2
29	71	F	A	247	>12	+	+	ND	13q-	265	98.0	1.5	2/3
30	50	F	B	269	>12	−	+	UM	13q-	195	92.0	6.0	2/2
31	81	M	B	281	<12	−	+	UM	13q-	52	91.6	3.7	2/2
32	58	M	A	274	ND	+	ND	ND	13q-	50	65.0	18.5	2/2
33	69	M	B	220	>12	+	ND	ND	+12	37	75.0	19.3	1/1
34	64	M	A	211	>12	+	+	M	13q-	52	90.0	8.1	2/2
35	69	M	A	203	>12	−	−	M	ND	57	91.3	5.5	2/2
36	62	M	B	176	<12	−	ND	ND	ND	105	96.0	3.5	2/2
37	93	M	B	264	ND	ND	ND	ND	ND	120	95.9	2.1	2/2
38	44	M	C	186	<12	−	−	M	13q-	387	95.0	5.0	2/2
39	78	M	B	338	<12	−	−	M	13q-	550	98.0	0.4	3/3
Med	62			220							94.7	3.9	102/126

Abbreviations: LDT, lymphocyte doubling time; IgVH, immunoglobulin heavy-chain variable; UM, unmutated; M, mutated; ND, not done; 13q-, deletion in band 13q14; 11q-, deletion in band 11q23; 17p-, deletion in band 17p13; +12, trisomy of chromosome 12; WBC, WBC count; eng, engrafted mice.

monoclonal antibodies. In some experiments, cell-surface antigens were first stained and fixed, followed by permeabilization of the plasma membrane (Cytofix/Cytoperm, Becton Dickinson) and staining of intracellular antigens. After washing, four-color flow cytometric analysis of human antigens was done on a Coulter Epics XL analyzer (Coulter Electronics). Erythrocyte lysis (Pharmlyse, Becton Dickinson) of the cells was done before staining. The following directly labeled antibodies were used for the characterization of human cells: CD45-cyanine dye (Cy5), CD19-phycoerythrin, CD5-FITC and CD23-energy coupled dye, λ light chain (FITC, Kallestad), κ light chain (FITC, Kallestad), CD38 phycoerythrin (Becton Dickinson), CD100 (FITC, Serotec), and survivin (FITC, R&D Systems) for CLL cells; CD45-Cy5, CD4-phycoerythrin, CD8-FITC, and CD3-energy coupled dye for human T cells. Antibodies were purchased from Beckman Coulter Immunotech except indicated otherwise. For the determination of ZAP-70, we used an indirect staining approach as previously described (5) using anti-ZAP-70 (clone 2F3.2, Upstate Biotechnology) as a primary antibody and goat-anti-mouse immunoglobulin-FITC (DAKO) as secondary antibody. Phycoerythrin-, phycoerythrin-cyanin 5.1–, energy coupled dye–, and FITC-conjugated mouse isotypic monoclonal antibodies served as controls and were included in all experiments.

Bromodeoxyuridine incorporation experiments. Analysis of 5-bromodeoxyuridine (BrdUrd) incorporation was done using the FITC BrdUrd Flow kit (PharMingen) after a single i.p. injection of BrdUrd (PharMingen; 1 mg/6 g of mouse weight within 5 days after transplantation) and admixture of 1 mg/mL BrdUrd (Sigma) to drinking water for 5 days within week 1 and week 3 each, after transplantation (6). Analysis for BrdUrd incorporation in recovered CLL cells was only done when splenic engraftment >1% CLL cells of total spleen cells was evident.

Fluorescence *in situ* hybridization analysis. To detect specific anomalies of the leukemic clone in chromosomal regions 11q, 13q, and 17p in cells recovered after transplantations, the following fluorescence-labeled DNA probes were used for interphase cytogenetic analyses: locus-specific identifier (LSI) ATM (11q23), LSI D13S319 (13q14), LSI p53 (17p13.1), and chromosome enumeration probe (CEP) 12 (centromere 12). All probes were purchased from Abbot Vysis. Sample preparation, fluorescence *in situ* hybridization (FISH), and counterstaining with 4,6-diamidino-2-phenylindole dihydrochloride were done as previously reported (5).

Histologic staining of spleen sections. Four-micrometer-thick sections of paraffin-embedded spleen sections were obtained and stained with H&E according to standard procedures. Additional serial sections were prepared for immunohistochemical investigation. Immunohistochemistry was done using the EnVision+ System peroxidase method (DAKO) with monoclonal mouse antibodies (immunoglobulin G) against human leukocyte common antigen (CD45, clones 2B11+PD7/26, DakoCytomation; dilution, 1:1,000), CD3 (clone F7.2.38, DakoCytomation; dilution, 1:100), CD20 (clone L26, DakoCytomation; dilution, 1:4,000), CD21 (clone 1F8), and Ki67 (clone BGX-297, ready to use, BioGenex).

For double immunohistochemistry, the same CD3 and CD20 antibodies and an additional Ki67 antibody were used (Ki67, clone SP6, DCS; dilution, 1:1,200). Antigen retrieval was carried out at 98°C for 10 min in a water bath (Target retrieval buffer, DAKO). The CD3/Ki67 and CD20/Ki67 double labelings were done in two steps. First, Ki67 labeling with an immunohistochemical staining technique based on a horseradish peroxidase (HRP)–labeled polymer that is conjugated to secondary antibodies (ZytoChemPlus HRP Polymer Kit, Zytomed Systems) was done. Staining was completed by an incubation with 3,3′-diaminobenzidine + substrate-chromogen (Zytomed Systems), which results in a brown-colored precipitate at the antigen site. Second, CD3 or CD20 labeling was done with an alkaline phosphatase–labeled polymer [ZytoChemPlus (AP) Polymer Kit, Zytomed Systems] and developed with a Permanent Red chromogenic substrate system (Zytomed Systems). At the end of the procedure, nuclei were counterstained with hematoxylin for 5 min.

***In situ* hybridization.** For the detection of a latent EBV infection by *in situ* hybridization, sections from paraffin-embedded tissue were analyzed. In brief, slides were dewaxed, rehydraded, and dried at 45°C. Afterward, they were pretreated with proteinase K for 25 min at 37°C. Two drops of EBV-specific FITC-labeled oligonucleotide probe [DAKO, Epstein-Barr Virus (EBER) PNA Probe/Fluorescein] were added to the tissue section and slides were covered with coverslips. The hybridization was carried out for 90 min at 55°C. After washing with diethyl pyrocarbonate water, oligonucleotide binding was indirectly detected with an anti-FITC antibody conjugated to alkaline phosphatase (DAKO, PNA ISH detection kit).

Statistical analysis. Data are presented as the mean ± SE unless otherwise specified. Statistical analysis was done using SPSS 13.0 for Windows (SPSS, Inc.). The significance of differences between groups was determined with the Friedman test (differences between the application routes and differences in CLL or T-cell engraftment within the different tissue compartments), the Kruskal-Wallis test (differences in engraftment according to stage), the Wilcoxon test (differences between the mean fluorescence intensities of survivin and CD100 expression of transplanted and engrafted CLL cells and differences in CLL or T-cell engraftment within the same compartment), or the Mann-Whitney *U* test [differences in engraftment according to lactate dehydrogenase (LDH), lymphocyte doubling time, or prognostic parameters], with $P \leq 0.05$ considered to be significant.

Results

Establishment of a NOD/SCID Xenotransplant Model of Human CLL

All in all, the transplantation of 43 primary human peripheral blood-derived CLL samples from 39 different CLL patients was investigated in a total of 167 NOD/SCID mice. The clinical characteristics of the patients are shown in Table 1.

In initial experiments using 5 different CLL samples and 35 NOD/SCID mice, the most suitable route for transplantation was determined by transplanting 1×10^8 CLL cells from the same sample either i.p. (n = 12 mice), i.v. (n = 12 mice), or via both routes (i.p. + i.v.; n = 11 mice). Figure 1*A* shows representative flow cytometry plots of CLL cells before transplantation and of human cells recovered from the bone marrow, spleen, and peritoneal cavity of a NOD/SCID animal showing that the recovered cells from all three compartments exhibited the $CD19^+CD5^+CD23^+$ immunophenotype characteristic of CLL cells. On quantitative analysis, the number of recovered CLL cells was significantly higher in the spleen and peritoneal cavity as compared with the bone marrow (Fig. 1*B*). Whereas CLL recovery in the murine spleen was higher following i.v. versus i.p. transplantation, cell recovery in the peritoneal cavity was mainly dependent on the i.p. route. Combination of both routes, however, yielded the best results (Fig. 1*B*).

We then proceeded to validate this model in a cohort of 39 CLL patients (Table 1). For these experiments, only the combined i.v. + i.p. injection route was used and a total of 126 mice were evaluated. In line with our previous results, analysis at week 4 revealed consistent engraftment of human $CD45^+$ cells in 37 of 39 (94.9%) experiments. The highest number of $CD45^+$ cells was detected in the murine spleens whereas cell recovery from bone marrow and peritoneal cavity was significantly lower (Fig. 1*C*; P = 0.00000001). Human T cells engrafted more efficiently than their leukemic counterparts, accounting for the majority of $CD45^+$ cells in the murine spleen and bone marrow (Fig. 1*C*). Of note, a reverse engraftment pattern was noted in the murine peritoneal cavity, where the number of CLL cells recovered after 4 weeks exceeded that of the accessory T cells (P = 0.038; Fig. 1*C*). In the peripheral blood, comparably low numbers of CLL cells were detected in 12 of 18 and 8 of 22 samples 2 and 4 weeks after transplantation, accounting for 1.1 ± 0.5% and 0.7 ± 0.3% of the total peripheral blood leukocytes at these time points. Again,

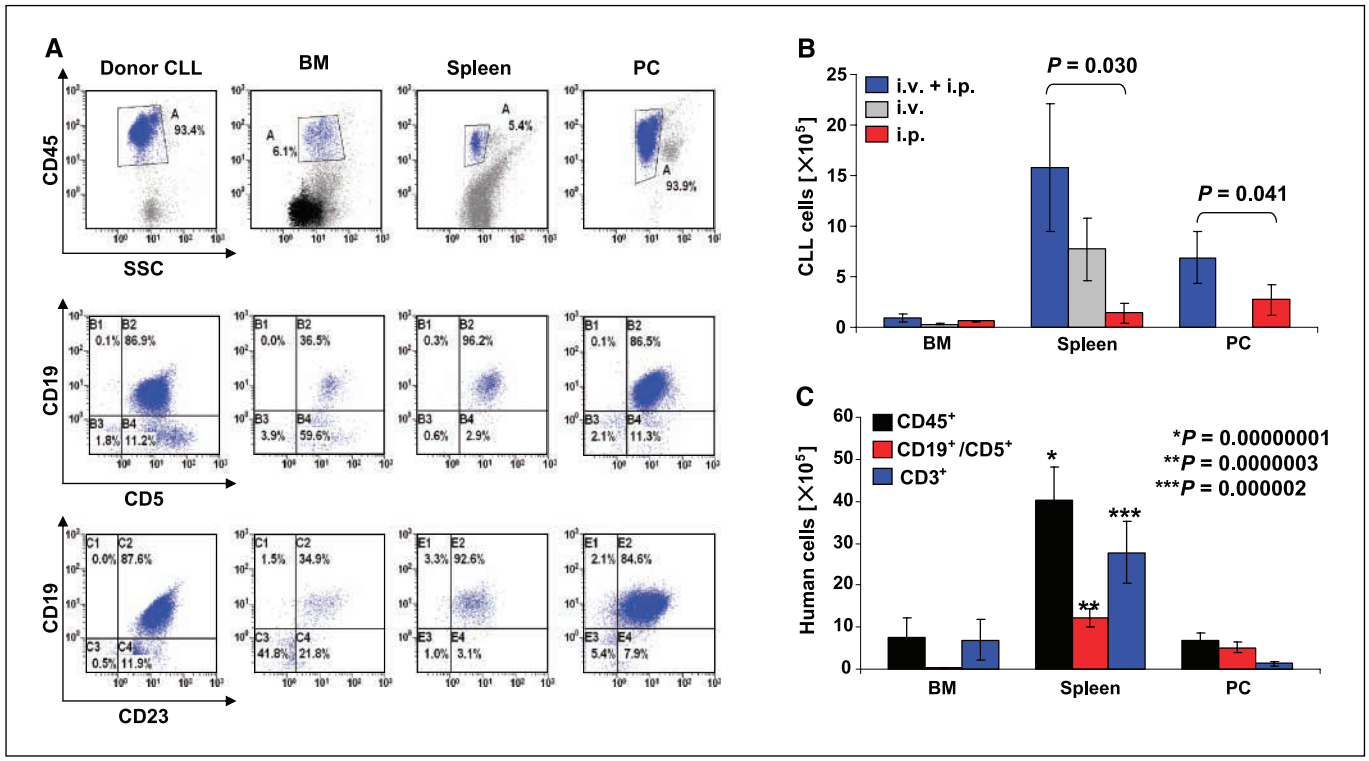

Figure 1. Human B-CLL cells recovered from bone marrow, spleen, and peritoneal cavity of NOD/SCID mice. *A,* representative flow cytometry plots of cells transplanted (*Donor CLL*) and cells recovered from bone marrow (*BM*), spleen, and peritoneal cavity (*PC*) of animals 4 wks after transplantation exhibit the CLL-typical $CD19^+CD5^+CD23^+CD45^+$ surface phenotype. *B,* quantitative recovery of human B-CLL cells 4 wks after transplantation of 1×10^8 PBMC i.p., i.v., or via both routes (i.p. + i.p.) in bone marrow, spleen, and peritoneal cavity of NOD/SCID mice. *C,* quantitative recovery of human $CD45^+$, B-CLL, or $CD3^+$ human T cells 4 wks after transplantation of 1×10^8 PBMC i.p. and i.v., respectively, in bone marrow, spleen, and peritoneal cavity of NOD/SCID mice. Evaluation of the model with a total of 39 different CLL samples using the i.p. + i.v. combination. Significantly higher engraftment for all three subpopulations could be shown for the spleen when compared with bone marrow or peritoneal cavity. *Columns,* mean; *bars,* SEM. *SSC,* side scatter.

higher engraftment rate and absolute number of human T cells were detected in the peripheral blood of the transplanted animals 2 weeks (17 of 17) and 4 weeks (14 of 22) after transplantation, accounting for $10.2 \pm 4.0\%$ and $6.6 \pm 3.5\%$ of the total peripheral blood leukocytes, respectively.

Taken together, these results suggest that murine splenic tissue offers a more supportive microenvironment for the engraftment of CLL PBMC than peritoneal cavity, bone marrow, and peripheral blood.

Individual reproducibility. To evaluate the reproducibility of our model in four individual patients showing high, moderate, low, or no splenic CLL cell recovery, transplantation was repeated at a later time point. Comparative analysis of human CLL cells recovered from the spleens in these four paired experiments showed reproducible recovery of CLL cells for individual patients, and 29.9×10^5 versus 19.6×10^5, 15.8×10^5 versus 15.4×10^5, and 2.2×10^5 versus 11.2×10^5 recovered cells, and no engraftment versus no engraftment were observed. To unequivocally confirm that the recovered $CD45^+CD19^+CD5^+CD23^+$ cells originated from the transplanted leukemic cell clones, we carried out comparative FISH and immunoglobulin light chain restriction analyses in a series of four cases with informative cytogenetic aberrations. Reassuringly, concordant results with both assays were observed in all of the four cases (Supplementary Fig. S1).

Time course of CLL cell engraftment. In a total of five experiments, the recovery of human CLL cells in the spleen as well as the peritoneal cavity of NOD/SCID mice was evaluated over a more extended time period. Whereas absolute numbers of recovered CLL cells remained relatively stable between weeks 4 and 8 (spleen, $5.5 \pm 3.2 \times 10^5$ versus $2.4 \pm 1.4 \times 10^5$; peritoneal cavity, $0.6 \pm 0.3 \times 10^5$ versus $3.2 \pm 2.9 \times 10^5$); at week 12, a substantial decline of cells was noted in the spleen ($0.6 \pm 0.3 \times 10^5$) as well as the peritoneal cavity ($0.2 \pm 0.1 \times 10^5$).

Histologic Analysis of Splenic Engraftment

In view of the fact that the highest absolute number of human cells was consistently observed in the murine spleens, we further investigated the histomorphologic appearance of these cells using H&E as well as immunohistologic staining of spleen sections. All in all, 46 mice transplanted with 15 different CLL samples were analyzed (Supplementary Table S1). Strikingly, a focal infiltration pattern of human lymphoid $CD45^+$ cells situated along the splenic arterioles was observed in the majority of animals (37 of 46; representing 14 of 15 CLL samples; Fig. 2*A*). On immunohistochemistry, the majority of cells in these focal aggregates exhibited a $CD20^+$ CLL phenotype ($88.3 \pm 3.6\%$; Fig. 2*B*), whereas a smaller proportion represented accessory $CD3^+$ T cells ($11.0 \pm 3.4\%$; Fig. 2*C*). In some cases, these focal aggregates consisted almost exclusively (>99%) of $CD20^+$ CLL cells (Supplementary Table S1). The majority of the H&E-stained lymphoid $CD20^+$ cells morphologically exhibited typical features of prolymphocytes: cells were larger than a normal lymphocyte and their nuclei contained finely distributed chromatin as well as small nucleoli (Fig. 2*D, arrows*). Besides this population, a fraction of paraimmunoblasts characterized by a nucleus containing a solid centrally located nucleolus was observed (Fig. 2*D, cones*). When the potential presence of

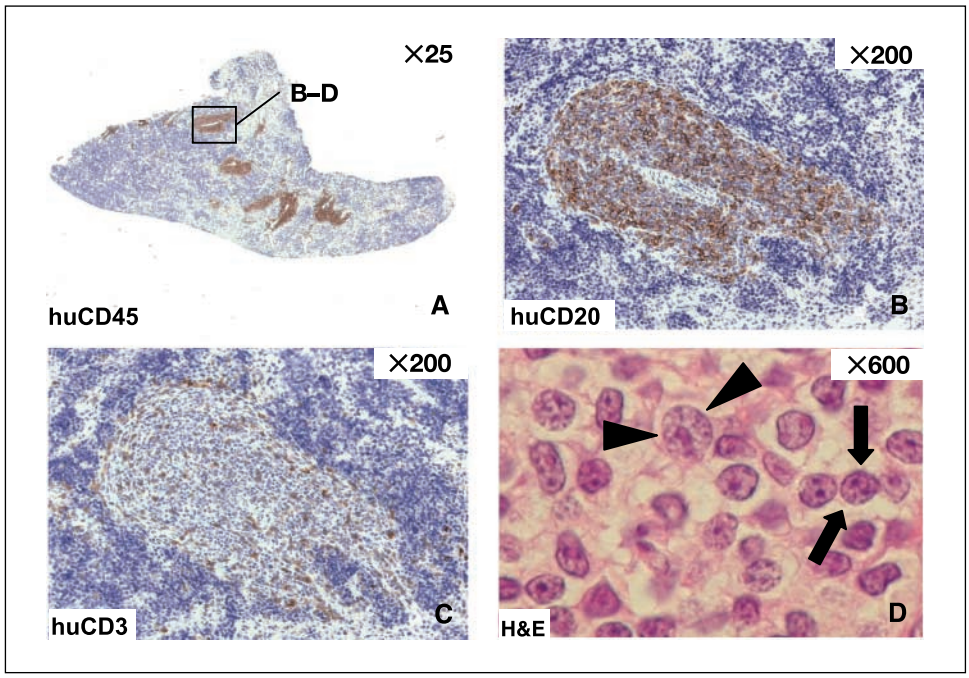

Figure 2. Histomorphologic appearance of recovered human cells in the murine spleen. *A,* focal aggregates of human CD45$^+$ cells clustering around splenic arterioles (×25 magnification). *B,* subpopulation analysis of focal aggregates reveals predominantly human CD20$^+$ CLL cells (×200 magnification) interspersed with a smaller population of human CD3$^+$ T cells (×200 magnification; *C*). *D,* focal aggregates of human cells compose predominantly two lymphoid populations, fitting the histologic criteria of prolymphocytes (→ ←) and paraimmunoblasts (► ◄).

human follicular dendritic cells within the splenic aggregates was evaluated by immunostaining of CD21, no follicular dendritic cells were detected.

A minority of animals (9 of 46; 6 of 15 CLL samples; Supplementary Table S1) showed a more diffuse infiltration pattern of human cells consisting mostly of CD3$^+$ T cells (72.5 ± 8.4%) and less frequently of CD20$^+$ CLL cells (27.5 ± 8.4%). Of note, histomorphologic analysis of spleen sections 12 weeks after transplantation frequently revealed a considerable amount of fibrosis with a consecutive loss of structural integrity of the murine splenic tissue, which was not detectable 4 weeks after transplantation. To rule out EBV-transformed lymphoma cells as the source of the recovered human cells in several experiments, additional *in situ* hybridization analysis for EBV-encoded RNAs was done

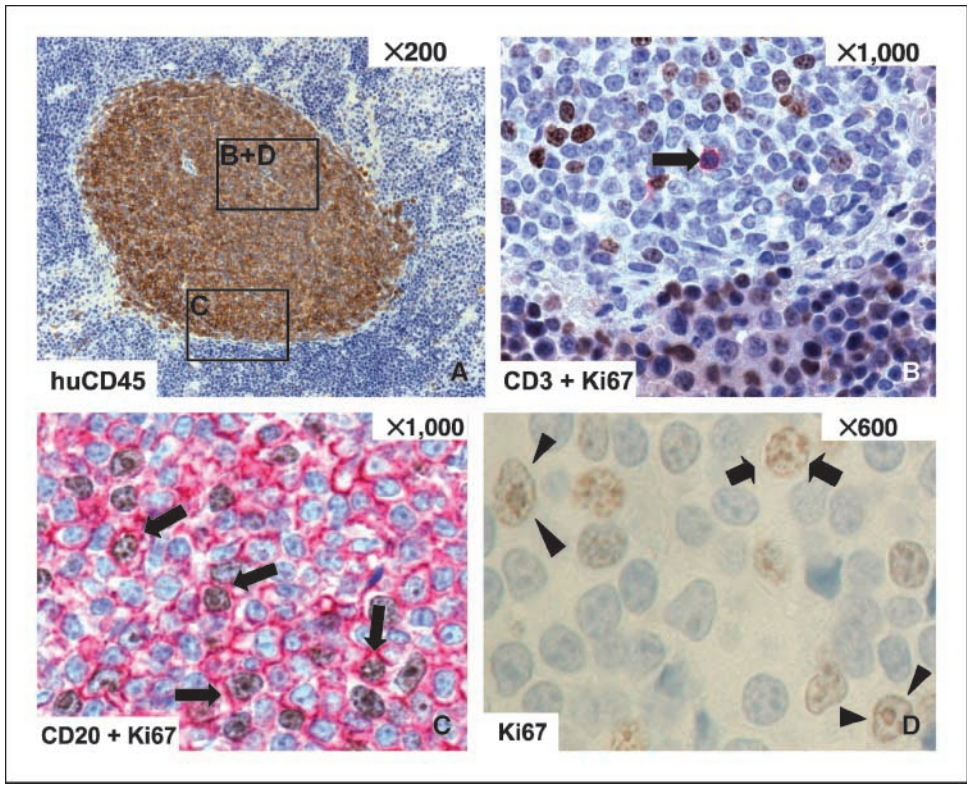

Figure 3. Immunohistologic characterization of CLL cells localized in focal aggregates in the spleens of NOD/SCID mice. Serial immunohistologically stained sections of a murine spleen showing focal engraftment of CD45$^+$ human lymphoid cells were investigated. *A,* a representative focal aggregate composed of human CD45$^+$ cells. *B* and *C,* double immunostaining of Ki67 (*brown*) and CD3 (*red*; *B*) or CD20 (*red*; *C*) identifies a single CD3$^+$ but Ki67$^-$ cell (*B*, →) but multiple CD20$^+$ cells coexpressing Ki67 (*C*, →) within the splenic focal aggregate. About 10% of the aggregate composing cells show Ki67 positivity (*C* and *D*). Ki67 staining seems to be restricted to cells with activated either prolymphocytic (→ ←) and/or paraimmunoblast (► ◄) phenotype (*D*).

(5 CLL samples, n = 10 mice), revealing no EBV-RNA–positive cells within the focal aggregates (data not shown).

CLL Cells Recovered from Murine Spleens Exhibit a Distinct Phenotype and Show Proliferative Activity

To further characterize the human CLL cells recovered from the NOD/SCID spleens, a panel of surface and intracellular marker molecules was used. Given the histologic similarities between the focal aggregates observed in our NOD/SCID model and the pseudofollicular proliferation centers described in human CLL (7), this analysis focused on marker molecules described as characteristic of CLL cells located in proliferation centers, survivin, and CD100 (8–10). In 23 mice presenting with focal aggregates in the spleen, consistently a substantial percentage of human CD45$^+$ cells (19.5 $\pm$ 2.7%) stained positive for Ki67. Analysis of focal aggregates composed almost exclusively (>99%) of CD20$^+$ CLL with only sporadic interspersed T cells indirectly confirmed that Ki67 was indeed expressed in CLL cells (data not shown). In addition, Ki67 expression in CLL cells and absence of Ki67 expression in human T cells could be shown directly by double immunostaining of Ki67 and CD20 as well as CD3 (Fig. 3*A*–*C*). Here, hardly any Ki67 staining was detected in human CD3$^+$ T cells (Fig. 3*B*), but coexpression of Ki67 and CD20 was evident in a substantial fraction of CLL cells recovered from the murine spleens (Fig. 3*C*). Of note, high-power magnification of splenic focal CLL aggregates revealed that the Ki67$^+$ cells exhibited morphologic features of either paraimmunoblasts or prolymphocytes (Fig. 3*D*).

Activation of CLL cells within proliferation centers has also been shown to result in increased expression of survivin, one of the inhibitor of apoptosis proteins, as well as up-regulation of the semaphorin protein family member CD100 (semaphorin 4D; refs. 8–10). As depicted in Supplementary Fig. S2, the same pattern of activation was observed in our CLL model. Of note, significant up-regulation of survivin (P = 0.028; Supplementary Fig. S2*B*) as well as CD100 (P = 0.043; Supplementary Fig. S2*D*) was detected in leukemic cells recovered from NOD/SCID spleens when compared with the initially transplanted CLL cells.

To further investigate the proliferative potential of human CLL cells recovered from NOD/SCID spleens, 5-bromodeoxyuridine (BrdUrd) incorporation during a 1- to 3-week *in vivo* exposure period was analyzed in five samples showing typical focal aggregates in the corresponding histomorphologic analyses. In

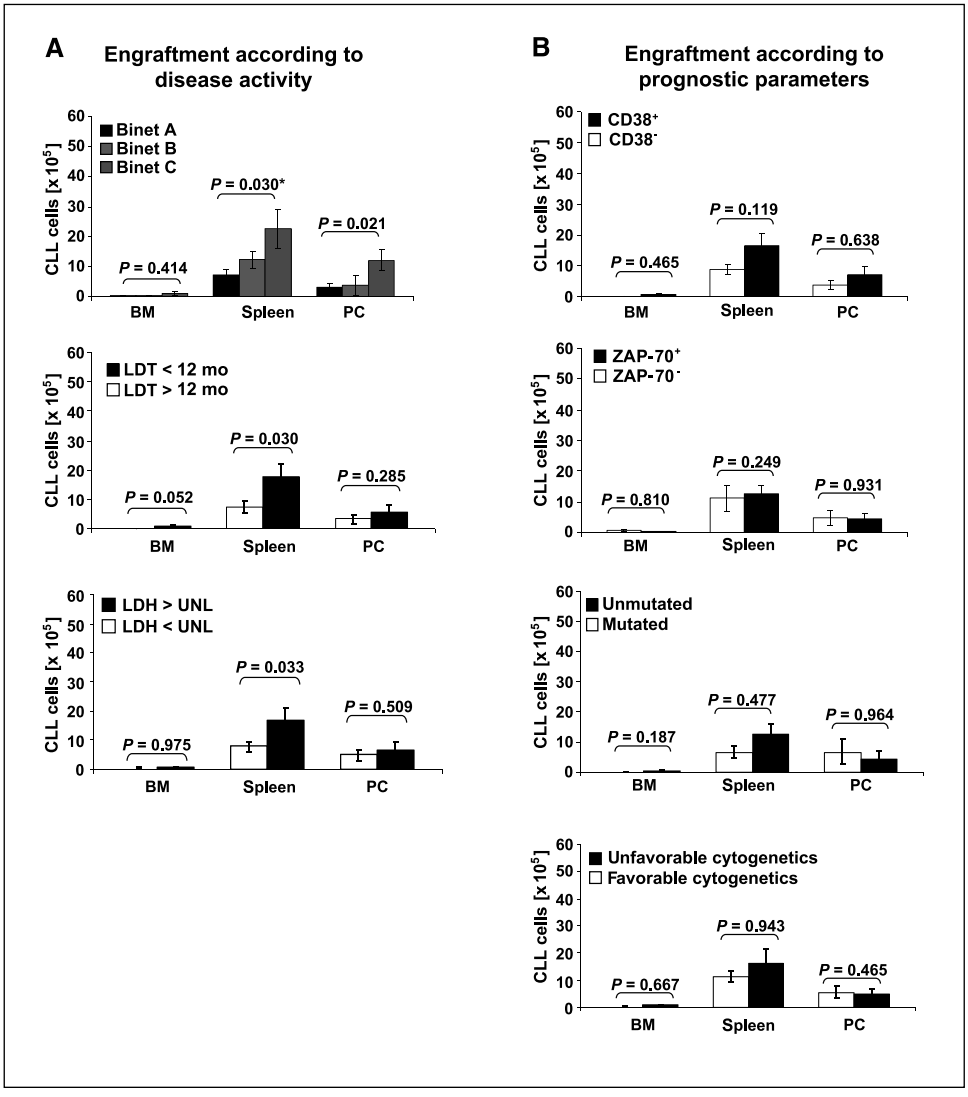

Figure 4. Recovery of human B-CLL cells with regard to disease activity and prognostic parameters. Quantitative recovery of B-CLL cells 4 wks after transplantation of 1 $\times$ 10^8 PBMC i.p. and i.v., respectively, in bone marrow, spleen, and peritoneal cavity of NOD/SCID mice. *A,* recovery of CLL cells was significantly correlated with parameters reflecting disease activity [e.g., Binet stage, lymphocyte doubling time (*LDT*), and LDH serum activity (*LDH*)]. *B,* samples obtained from poor prognosis patients as defined by expression of CD38, ZAP-70, unmutated IgVH genes, or unfavorable cytogenetics generally showed a higher leukemic cell engraftment than CLL cells isolated from patients with good prognosis. However, the observed differences did not reach statistical significance (P > 0.05).

these experiments, 6.7% to 25.0% of the recovered splenic CLL cells stained positive for BrdUrd (Supplementary Fig. S3), indicating that a significant proportion of splenic CLL cells located within splenic aggregates had entered the cell cycle during the BrdUrd exposure period.

Correlation of Splenic CLL PBMC Engraftment with Clinical and Molecular Disease Parameters

We then proceeded to correlate splenic CLL PBMC engraftment with the disease characteristics observed in individual patients at the time of transplantation (Fig. 4). Here, we found that parameters reflecting disease activity (e.g., Binet stage, lymphocyte doubling time, and LDH serum activity) exhibited a significant positive correlation with CLL cell engraftment (Fig. 4*A*). Disease stage also affected the histologic appearance of the transplanted cells in the murine spleens in that samples from Binet stage C patients exclusively engrafted in a follicular pattern. By contrast, all of the nine cases with a diffuse infiltration pattern were observed in samples obtained from Binet stage A and B patients (Supplementary Table S1). In line with these findings, samples obtained from poor-prognosis patients, as defined by expression of CD38 (8, 11–13), ZAP-70 (5, 14–17), unmutated IgVH genes (11, 18, 19), or high-risk cytogenetics (20), generally showed a higher leukemic cell engraftment than CLL cells isolated from patients with good prognosis (Fig. 4*B*). However, the observed differences failed to reach statistical significance, suggesting that the model may better reflect disease activity at the time of venipuncture rather than the long-term clinical course of individual cases.

Effects of Accessory T Cells on Splenic CLL Cell Recovery

Interestingly, increased leukemic B-cell engraftment in advanced disease stages inversely correlated with the number of recovered accessory T cells (Fig. 5), suggesting that the biological properties of CLL T cells may change in the course of the disease. To further define the role of accessory human T cells in this model, comparative transplantation experiments using T cell–depleted and T cell–enriched grafts were done. In line with the results shown in Fig. 5, we found that T cells isolated from patients with advanced/active disease seemed to increase leukemic cell recovery as compared with T cells obtained from patients with early/inactive disease (Supplementary Table S2). However, these potentially interesting findings are limited by the small number of patients analyzed and thus need to be confirmed in a larger series. Furthermore, these experiments did not reveal a consistent effect of cotransplanted T cells on either histomorphologic appearance (focal aggregate formation) or survivin and CD100 expression by the leukemic cells (data not shown).

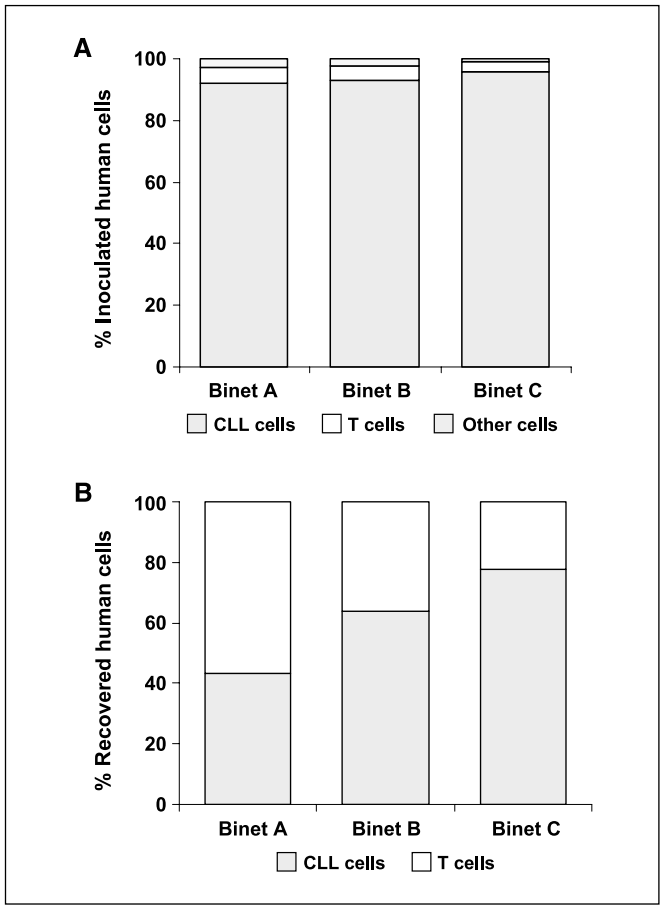

Figure 5. CLL cells derived from advanced-stage donors have a higher capacity to engraft in NOD/SCID spleens. *A,* cellular composition of inoculated PBMC as analyzed by flow cytometry. No significant differences in the content of CLL cells and accessory T cells were noted in PBMC samples derived from patients with different Binet stages. *B,* the ratio of engrafted human CLL and accessory T cells depends on the disease stage.

Discussion

We here describe a novel and robust *in vivo* model of human CLL using NOD/SCID mice as recipients of primary peripheral blood-derived CLL cells. In this model, we show reproducible and stable recovery of PBMC from CLL patients over a time span of 8 weeks after transplantation. Comparing different routes of transplantation, the highest number of human $CD45^+$ cells was detected in the murine spleen followed by the peritoneal cavity, bone marrow, and peripheral blood, suggesting that splenic tissue may offer the most suitable microenvironment for the transplanted cells.

Given that the highest number of engrafted human cells was observed in the murine spleen, we aimed to further investigate the morphologic and functional characteristics of these cells in this tissue compartment. Histomorphologic evaluation of spleen sections revealed focal aggregates of $CD45^+$ human cells consisting of both CLL and accessory T cells, which were clustered around splenic arterioles. At higher magnification, these focal aggregates were found to contain a mixture of paraimmunoblasts, prolymphocytes, and interspersed small lymphocytes. Further immunohistochemical evaluation showed that the prolymphocytic and paraimmunoblastic cells exhibit a $CD20^+CD23^+CD5^+$ phenotype and that a substantial proportion of these cells stain positive for the proliferation marker Ki67. The proliferative potential of these cells was confirmed by BrdUrd DNA incorporation experiments, which unequivocally showed that a substantial proportion of the transplanted CLL cells entered the cell cycle during the 4-week posttransplant period. Consistent with their proliferative potential and their "activated morphology," these cells were found to express the B-cell activation markers survivin and CD100, as detected by multiparameter flow cytometry. Both of these molecules have previously been shown to exert prosurvival effects in CLL cells and may play an important functional role in the molecular

pathogenesis of the disease (8–10). Whereas, to our knowledge, this is the first detailed report on the occurrence of splenic focal aggregates following the transplantation of CLL cells into mice, this is probably not a unique characteristic of CLL cells as previous work by Burakova et al. (21) has shown that transplanted normal human PBMC form follicles in the spleen and lymph nodes of SCID mice.

Clearly, the most important finding of this study is that the engraftment capacity of leukemic cells closely correlated with the disease characteristics observed in individual patients at the time of transplantation. In line with data published by the Reisner group (3, 4), we found that transplantation of PBMC obtained from patients in stage Binet A resulted in marked i.p. engraftment of human T cells, whereas only few leukemic cells were recovered from the peritoneal cavity of the recipient animals. Conversely, infusion of samples from donors with Binet C disease led to the predominant engraftment of tumor cells compared with a low number of accessory T cells. Importantly, using the combined i.v./i.p. transplantation route, which has previously not been used in this experimental setting, we observed a similar disease stage–dependent engraftment profile in the murine spleen and peritoneal cavity. However, absolute human cell recovery was higher in the murine spleen as compared with peritoneal cavity, raising the possibility that using splenic CLL cell engraftment as readout may be advantageous due to a potentially higher sensitivity of the assay system. Of note, disease stage and cellular composition of the human graft also affected the histologic appearance of the transplanted cells in the murine spleens in that samples from Binet stage C patients exclusively engrafted in a follicular pattern (Supplementary Table S 1). By contrast, all of the nine cases with a diffuse infiltration pattern were observed in samples obtained from Binet stage A and B patients. Furthermore, we found that parameters reflecting disease activity other than Binet stage [ref. 22; e.g., lymphocyte doubling time (23–25) and LDH serum activity] also exhibited a significant positive correlation with CLL cell engraftment. Similarly, when samples were grouped according to the expression/presence of the molecular risk factors (19) CD38 (13), ZAP-70 (5, 26), IgVH mutation status (11, 18), and karyotype (20), the prognostically unfavorable group generally showed a higher leukemic cell engraftment than CLL cells isolated from patients with good prognosis. However, the observed differences failed to reach statistical significance, suggesting that the model may better reflect disease activity at the time of venipuncture rather than the long-term clinical course of individual cases.

Taken together, leukemic cells from advanced-stage patients have a higher engraftment potential than early-stage CLL cells, whereas T cells derived from patients with advanced disease engraft less efficiently than their counterparts obtained from Binet stage A patients. This mutually exclusive pattern of engraftment first described by Shimoni et al. (4) raises the possibility that T cells may at least partly control the expansion of the tumor cell clone *in vivo*. Our data are compatible with the concept that T cells isolated from early-stage patients may be capable of suppressing tumor cell growth (27, 28) whereas T cells from Binet stage C may have lost their antineoplastic immunosurveillance function (29, 30). In support of this hypothesis, we found that addition of autologous T cells purified from Binet stage A patients reduces splenic leukemic cell engraftment whereas addition of T cells from patients with progressive/advanced disease increases leukemic cell recovery from murine spleens. In this context, it is worth noticing that T cells of CLL patients with indolent disease have been shown to exhibit a lower production of leukemic cell survival–promoting cytokines as compared with T cells from patient with advanced disease (31, 32).

In conclusion, our data show that PBMC from CLL patients can be effectively engrafted into NOD/SCID mice. Using combined i.v./i.p. transplantation, the highest number of engrafted cells is detected in the murine spleen, where these cells can be conveniently quantified and subjected to further functional analysis. Our finding that CLL cells obtained from advanced-stage patients with elevated LDH serum activity and short lymphocyte doubling time exhibit a higher engraftment potential as compared with samples derived from donors with indolent disease suggests that our model reflects the heterogeneity and important clinical features of the disease. Thus, we suggest to further evaluate this model as a tool for preclinical drug testing and the investigation of the pathophysiology of CLL.

Acknowledgments

Received 3/30/2007; accepted 6/29/2007.

Grant support: Förderverein Innere Klinik und Poliklinik (Tumorforschung) e.V. and Deutsche José Carreras Leukämie-Stiftung grant DJCLS R 06/24 (J. Dürig and T. Moritz).

The costs of publication of this article were defrayed in part by the payment of page charges. This article must therefore be hereby marked *advertisement* in accordance with 18 U.S.C. Section 1734 solely to indicate this fact.

We thank A. Feldmann, W. Stellberg, A. Führer, and B. Friedmann for excellent technical help, K. Metz for histopathologic advice, and J. Cancelas and D.A. Williams for helpful discussions.

This work is dedicated to Prof. G. Brittinger on the occasion of his 75th birthday.

References

1. Hummel JL, Lichty BD, Reis M, Dube I, Kamel-Reid S. Engraftment of human chronic lymphocytic leukemia cells in SCID mice: *in vivo* and *in vitro* studies. Leukemia 1996;10:1370–6.
2. Kobayashi R, Picchio G, Kirven M, et al. Transfer of human chronic lymphocytic leukemia to mice with severe combined immune deficiency. Leuk Res 1992;16:1013–23.
3. Shimoni A, Marcus H, Canaan A, et al. A model for human B-chronic lymphocytic leukemia in human/mouse radiation chimera: evidence for tumor-mediated suppression of antibody production in low-stage disease. Blood 1997;89:2210–8.
4. Shimoni A, Marcus H, Dekel B, et al. Autologous T cells control B-chronic lymphocytic leukemia tumor progression in human->mouse radiation chimera. Cancer Res 1999;59:5968–74.
5. Schroers R, Griesinger F, Trumper L, et al. Combined analysis of ZAP-70 and CD38 expression as a predictor of disease progression in B-cell chronic lymphocytic leukemia. Leukemia 2005;19:750–8.
6. Hock H, Hamblen MJ, Rooke HM, et al. Gfi-1 restricts proliferation and preserves functional integrity of haematopoietic stem cells. Nature 2004;431:1002–7.
7. Bonato M, Pittaluga S, Tierens A, et al. Lymph node histology in typical and atypical chronic lymphocytic leukemia. Am J Surg Pathol 1998;22:49–56.
8. Deaglio S, Vaisitti T, Bergui L, et al. CD38 and CD100 lead a network of surface receptors relaying positive signals for B-CLL growth and survival. Blood 2005;105:3042–50.
9. Granziero L, Circosta P, Scielzo C, et al. CD100/Plexin-B1 interactions sustain proliferation and survival of normal and leukemic $CD5^+$ B lymphocytes. Blood 2003;101:1962–9.
10. Granziero L, Ghia P, Circosta P, et al. Survivin is expressed on CD40 stimulation and interfaces proliferation and apoptosis in B-cell chronic lymphocytic leukemia. Blood 2001;97:2777–83.
11. Damle RN, Wasil T, Fais F, et al. Ig V gene mutation status and CD38 expression as novel prognostic indicators in chronic lymphocytic leukemia. Blood 1999;94:1840–7.
12. Deaglio S, Capobianco A, Bergui L, et al. CD38 is a signaling molecule in B-cell chronic lymphocytic leukemia cells. Blood 2003;102:2146–55.
13. Durig J, Naschar M, Schmucker U, et al. CD38 expression is an important prognostic marker in chronic lymphocytic leukaemia. Leukemia 2002;16:30–5.
14. Del Principe MI, Del Poeta G, Buccisano F, et al. Clinical significance of ZAP-70 protein expression in B-cell chronic lymphocytic leukemia. Blood 2006;108:853–61.

15. Durig J, Nuckel H, Cremer M, et al. ZAP-70 expression is a prognostic factor in chronic lymphocytic leukemia. Leukemia 2003;17:2426–34.
16. Hamblin TJ. Predicting Progression-ZAP-70 in CLL. N Engl J Med 2004;351:856–7.
17. Orchard JA, Ibbotson RE, Davis Z, et al. ZAP-70 expression and prognosis in chronic lymphocytic leukaemia. Lancet 2004;363:105–11.
18. Hamblin TJ, Davis Z, Gardiner A, Oscier DG, Stevenson FK. Unmutated Ig V(H) genes are associated with a more aggressive form of chronic lymphocytic leukemia. Blood 1999;94:1848–54.
19. Shanafelt TD, Geyer SM, Kay NE. Prognosis at diagnosis: integrating molecular biologic insights into clinical practice for patients with CLL. Blood 2004;103:1202–10.
20. Dohner H, Stilgenbauer S, Benner A, et al. Genomic aberrations and survival in chronic lymphocytic leukemia. N Engl J Med 2000;343:1910–6.
21. Burakova T, Marcus H, Canaan A, et al. Engrafted human T and B lymphocytes form mixed follicles in lymphoid organs of human/mouse and human/rat radiation chimera. Transplantation 1997;63:1166–71.
22. Binet JL, Auquier A, Dighiero G, et al. A new prognostic classification of chronic lymphocytic leukemia derived from a multivariate survival analysis. Cancer 1981;48:198–206.
23. Molica S, Alberti A. Prognostic value of the lymphocyte doubling time in chronic lymphocytic leukemia. Cancer 1987;60:2712–6.
24. Montserrat E, Sanchez-Bisono J, Vinolas N, Rozman C. Lymphocyte doubling time in chronic lymphocytic leukaemia: analysis of its prognostic significance. Br J Haematol 1986;62:567–75.
25. Vinolas N, Reverter JC, Urbano-Ispizua A, Montserrat E, Rozman C. Lymphocyte doubling time in chronic lymphocytic leukemia: an update of its prognostic significance. Blood Cells 1987;12:457–70.
26. Rassenti LZ, Huynh L, Toy TL, et al. ZAP-70 compared with immunoglobulin heavy-chain gene mutation status as a predictor of disease progression in chronic lymphocytic leukemia. N Engl J Med 2004;351:893–901.
27. Decker T, Flohr T, Trautmann P, et al. Role of accessory cells in cytokine production by T cells in chronic B-cell lymphocytic leukemia. Blood 1995;86:1115–23.
28. Mellstedt H, Choudhury A. T and B cells in B-chronic lymphocytic leukaemia: Faust, Mephistopheles and the pact with the Devil. Cancer Immunol Immunother 2006;55:210–20.
29. Aguilar-Santelises M, Mellstedt H, Jondal M. Leukemic cells from progressive B-CLL respond strongly to growth stimulation *in vitro*. Leukemia 1994;8:1146–52.
30. Dadmarz R, Rabinowe SN, Cannistra SA, Andersen JW, Freedman AS, Nadler LM. Association between clonogenic cell growth and clinical risk group in B-cell chronic lymphocytic leukemia. Blood 1990;76:142–9.
31. Rossmann ED, Jeddi-Tehrani M, Osterborg A, Mellstedt H. T-cell signaling and costimulatory molecules in B-chronic lymphocytic leukemia (B-CLL): an increased abnormal expression by advancing stage. Leukemia 2003;17:2252–4.
32. Rossmann ED, Lewin N, Jeddi-Tehrani M, Osterborg A, Mellstedt H. Intracellular T cell cytokines in patients with B cell chronic lymphocytic leukaemia (B-CLL). Eur J Haematol 2002;68:299–306.